FAILURE BEHAVIOUR OF WIDE PLATES WITH DIFFERENT GEOMETRIES AND ITS PREDICTION BASED ON FRACTURE MECHANICS

R. Hubo*, W. Dahl* and H. Ehrhardt**

The failure behaviour of wide plates has been analysed concerning their deformation- and fracture behaviour. Significant differences for different defect types and overall plate dimensions were demonstrated. Characteristic transition temperatures describing a change in the micromechanism or in the failure behaviour were determined experimentally and predicted with failure assessment concepts like the CTOD-design-curve approach and the FAD-diagram. The assessment routines lead to a conservative prediction of the wide plate behaviour.

INTRODUCTION

The failure behaviour of large structural components has to be checked to garantee the safety of the entire structure under service conditions. Since testing of the component itself is an expensive way to get the necessary informations smaller specimens, simulating the real component as far as possible, have to be examined. Wide plates are used to simulate a simple, tension loaded structural element. Artifical defects like fatigue cracks or machined notches induce areas of high constraint to get a description of the failure behaviour under severe loading conditions.

Investigations of wide plates at the IEHK /1,2/ are concentrated on two topics: The description of the deformation and failure behaviour of wide plates under service like loading conditions and the application of concepts trying to predict the failure behaviour. About 600 wide plate tests with different plate and defect geometry have been performed. From the wide range of geometries

* Institute of Ferrous Metallurgy, Technical University Aachen, Intzestr. 1, D-5100 Aachen, FRG

** AKZO (ENKA AG, Heinsberg-Oberbruch, Steelkord plant)

the results of tests with centre notch/centre crack, double edge notch and single surface notch will be presented.

MATERIAL AND WIDE PLATE GEOMETRY

Fe 510 steel plates of 30 mm thickness were used for these investigations. Table 1 shows the chemical composition of the steel. Besides the standard concentration of C, Si, Mn, P and Al the material showed a very low sulphur content. The results of mechanical testing at room temperature are summarized in table 2. The yield strength and the tensile strength were 401 MPa and 594 MPa respectively, the upper shelf charpy value was 200 J with a transition temperature $T_{50\%CVNmax}$ of 236 K.

Figure 1 shows the 3 different types of defects which have been used to vary the constraint in the plates. Centre notched or centre cracked (CNT, CCT), double edge notched (DENT) and single surface notched (SSNT) tension specimens were tested under displacement control at different temperatures between 183 K and room temperature with a cross head speed of 2 mm/min. The notches had a notch tip radius of 0.1 mm. A detailed description of the wide plate design is shown in table 3. The plate width was 300 mm except for two series of DENT-specimens having a width of 600 mm. The 2a/W-ratio was varied from 0.1 to 0.5 for CNT- and 0.1 to 0.8 for DENT-specimens. CCT-specimens with a fatigue crack instead of a notch were tested in addition. The SSNT-specimens had 2a/W-ratios from 0.2 to 1.0 and a/t-ratios between 2/15 and 2/3.

DEFORMATION BEHAVIOUR

The development of plastically deformed areas over the cross section of a wide plate can be observed at the surface of the specimen. Figure 2 shows the development of plastic zones in a CNT-/CCT-specimen together with a schematic stress-elongation-curve of a wide plate test under displacement control. Steels with upper and lower yield point show as the first step (point A of the stress-elongation-curve) contained yielding with sharp sliplines on the plate surface. The sliplines reach the edges of the plate at point B, where the plastic limit load is reached. For this type of specimens the plastic limit load is equal to the product of yield strength σ_{YS} at the test temperature times net section. The V-shaped section in front of the defect tip is furtheron deformed with increasing load (C and D). Strain hardening and reduction of cross section by stable crack growth are the dominating factors until the maximum stress is reached (plastic collapse load). Wide plates with small defects may also show gross-section-yielding on a stress level of point B.

This deformation pattern is typical for fully plastic specimen

behaviour and is independent from defect tip radius (notch or crack), defect length 2a and plate width W. Differences result only from the test temperature. At the fracture of the specimen characteristic points on the stress-elongation-curve are reached, e.g. point A for linear-elastic behaviour (brittle failure) at very low test temperatures.

The deformation of DENT-specimens is completely different from that of CNT-specimens (see figure 3). The sliplines originate from both defect tips A and the net section is completely pastified when the load is increased up to the yield point of the plate (B). In contrast to the CNT-/CCT-specimens the plastic limit load is not equal to the load calculated with the yield strength of the material but a constraint factor has to be taken into account. Based on the test results a plastic limit load equation for DENT-specimens under plane stress conditions has been derived:

$$F_{pll} = \sigma_{YS} [(W-2a) \cdot B] \left[1 + 0.1 \cdot \frac{2a}{W}\right] \qquad (1)$$

This constraint factor (last term of equation (1)) is different from what is proposed in the literature /3/. The further deformation is not concentrated on a special area of the plate, as could be shown for the CNT-(CCT-specimen, but is spreading away from the net-section into the adjacent areas (C and D). Strain hardening and stable crack growth is observed mainly in front of the defect tips. Differences resulting from geometry variations were not found beside the above mentioned change of constraint with increasing 2a/W-ratio. The influence of the test temperature is the same as found for the CNT-/CCT-specimens.

The deformation process of a SSNT-specimen is shown in figure 4. The left part shows the deformation in the notched and the right part that of the unnotched surface of the wide plate. Similarities to the deformation of CNT-/CCT-specimens could be shown like the sliplines starting from the end of the defect with an angle of about 45° to the ligament. In the centre of the wide plate sliplines can also be observed on the unnotched specimen surface. They originate from the defect tip spread through the thickness and reach the plate surface with an angle of about 45°. For 2c/W-ratios smaller than 1.0 two V-shaped areas of different orientations exist overlapping with increasing load. The stress at the plastic limit load is nearly independent from the wide plate geometry as observed for the CNT-/CCT-specimens. Areas with higher local constraint were only located directly in front of the defect tip. This influence is fully compensated by free deformation of the opposite surfaces.

CHARACTERISATION OF THE FAILURE BEHAVIOUR WITH TRANSITION TEMPERATURES

Depending on the test temperature different specimen behaviour can be observed. Figure 5 shows the deformation and fracture behaviour

of ferritic-perlitic steels with upper and lower yield point over a large temperature range. In the upper part the occurance of the micromechanisms of fracture - shear and cleavage fracture - are illustrated whereas the lower part shows load-elongation-curves which are characteristic for different test temperatures. In the centre the curves for the maximum stresses and for the yield stresses of tests at different temperatures are demonstrated. With this diagram characteristic transition temperatures can be evaluated /4, 5, 6/, defined by a change of the specimen behaviour or of the dominating micromechanism. Tgy (general yield) characterizes the transition from brittle to ductile specimen behaviour. At temperatures below Tgy brittle failure is observed whereas above Tgy the plastic limit load is reached and exceeded. The temperature Ti (initiation) is characterized by the first occurance of stable crack propagation. A change from stable to instable crack growth can still occur after some stable crack growth in a temperature range of 30 K to 50 K above Ti.

The exact determination of these transition temperatures needs a lot of tests at and around these temperatures. By wide plate tests being a very expensive way of material testing only a range can be determined where these temperatures can be found.

In figure 6 the transition temperature Tgy is shown as a function of defect type and geometry.

For CNT-specimens (6a) Tgy was determined at about 200 K and is not influenced by the defect length as long as the 2a/W-ratio is smaller than 0.3. For very small defects (less than 0.1) Tgy will presumably decrease, because the deformation behaviour of the wide plate is then very similar to a defect free specimen. A temperature shift of about 20 K to higher temperatures was only observed for the 2a/W-ratio of 0.5. The influence of notch tip acuity is very strong. Tgy of the CCT-specimens is about 20 K higher then that of CNT-specimens.

Comparing Tgy of CNT- and DENT-specimens (6b) of the same plate width, the CNT-specimens show sligtly lower transition temperatures for 2a/W-ratios up to 0.5 where Tgy is nearly the same for both types of specimens. For larger 2a/W-ratios in DENT-specimens Tgy is strongly decreasing. This is a point of current investigations.

An increase of plate width from 300 mm to 600 mm shifts Tgy about 30 K to higher temperatures (DENT-specimens). Further investigations should show, if Tgy can still be increased with increasing width or reaches an upper limit.

Figure 6c shows Tgy of SSNT-specimens as a function of the 2c/W-ratio for different a/t-ratios. The behaviour of SSNT-specimens with a a/t-ratio of 2/15 was ductile even at low test temperatures so that Tgy could not be determined. The specimens with a a/t-ratio of 0.5 showed a significantly more unfavourable transition behaviour than the test series with smaller and larger a/t-ratios. In particular for the specimens with a 2c/W-ratio of 1.0 and a/t = 0.5 the differences are quite large. This could be explained by

inhomogenities of the microstructure in the centre of the plate thickness, as they were found by metallographic examinations and also in Charpy tests.

Comparing all specimen types with equal plate width the SSNT-specimens show the lowest Tgy whereas for the DENT-specimens the highest Tgy have been evaluated. The maximum difference was about 40 K.

The transition temperature Ti is shown in figure 7 for all types of specimen. For wide plates with through thickness defects (CNT-/CCT-/DENT-specimens) Ti is independent of the 2a/W-ratio, defect tip acuity and specimen width. All values lie in a small scatter band between 243 K and 253 K. For the SSNT-specimens different transition temperatures Ti were determined the highest ones for a/t-ratios of 0.5 and the lowest ones for the smallest crack depth (a/t = 2/15). As already mentioned above these differences can be explained by inhomogenities over the plate thickness in particular unfavourable material properties in mid thickness of the plates.

PREDICTION OF TRANSITION TEMPERATURES BASED ON FRACTURE MECHANICS INVESTIGATIONS

Fracture mechanics concepts offer the possibility to assess defects in a given structure. A critical defect length or a critical load can be evaluated for a (given) situation. Since the material properties - strength and toughness - depend on temperature the analysis of the structural behaviour leads to different results for different temperatures. In this way the transition temperature Tgy for the change from brittle to ductile structure behaviour can be determined. The transition temperature Ti is nearly independent of geometry for equal thickness and loading rate and should be predicted by small scale tests with through thickness defect and equal specimen thickness.

Prediction of the transition temperature Ti

The transition temperature Ti is not influenced by the plate or the defect geometry as long as the defect orientation is equal for different specimen types (CNT-/CCT-/DENT-, see figure 7a,b). A comparison of the transition temperature Ti evaluated in fracture mechanics tests and in wide plates is demonstrated in figure 8 for the tested Fe 510 steel and a variety of other structural steels. In all cases defect orientation loading rate and specimen thickness were equal. Both temperatures are in good agreement so that the value from the small scale test seems to be transferable to the component like wide plate as long as the local constraint in front of the defect tip is equal in both kinds of tests.

Analysis based on the CTOD-Design-Curve-Approach

The CTOD-Design-Curve-Approach as proposed by Dawes et al. /7, 8/ can be used to predict the failure behaviour of wide plates based on the crack tip opening displacement (CTOD). Equation (2) describes a limit curve for 2a/W-ratios smaller than 0.5 and net section stresses lower than the yield stress.

$$\phi = \left[\frac{\sigma_1}{\sigma_{ys}}\right]^2 \left[1 - \frac{2a_{max}}{W}\right]^{-1} \qquad (2)$$

The mentioned restrictions allow an application of the concept only under contained yield conditions. Figure 9b shows the assessment of wide plates, which failed without reaching the plastic limit load with the conventional CTOD-Design-Curve-Diagram. The SSNT-defect geometry has been recategorized according to PD 6493 /9/.
The predictions were always on the safe side independent from specimen geometry. In figure 10a a comparison of the net-section-stress predictions of the CTOD-Design-Curve-Approach and the experimental results at different temperatures is shown for DENT-specimens with a 2a/W = 0.1. The prediction of Tgy is conservative and this trend is underlined by figure 10b where a comparison of calculated (CTOD) and experimentally determined Tgy is presented. A safety distance of 20 K to 30 K between calculated and experimental value is found. For the precracked test serie the prediction for the Tgy is nearly equal to the experimentally determined value.

Analysis based on the Failure Assessment diagram

The failure assessment diagram (CEGB, R6-Method, /10/) has been developed to evaluate both, brittle and ductile behaviour of a structure for given geometry and loading conditions. The transition from linear-elastic to plastic structural behaviour is described by a limit curve, which is independent from geometry:

$$K_r = [1 - 0.14\ L_r^2]\ [0.3 + 0.7\ \exp(-0.65\ L_r^6)]$$

The calculation of the K_r-value was performed based on fracture mechanics material parameters, which were used directly (K_{Ic}) or transformed formaly from J-Integral-values. The Failure Assessment Diagram in figure 11 presents the analysis for the majority of the tested wide plates. Option 1 and Category 1 were used for the assessment and lead to safe predictions for all tests with different safety factors. The L_r-value was determined with different limit load equations (I,II,III, see figure 11). In some cases the equations I and II from the literature /3/ can lead to unsafe predictions (see figure 12a). The equation III (see chapter 3) leads to

a conservative estimation of the failure behaviour. The comparison of calculated (R6-Method (equation II)) and experimentally determined Tgy shows again a safe prediction with a temperature difference of 20 K or more (see figure 12b).

CONCLUSIONS

The deformation behaviour of wide plates, which has been demonstrated for three types of specimens, CNT-/CCT-, DENT- and SSNT-specimens, depends strongly on the type of specimens. The same tendency was found for the transition from brittle to ductile specimen behaviour. The characterisation of this transition can be done with the experimentally determined transition temperature Tgy or with Tgy calculated with failure assessment methods like the CTOD-Design-Curve-Approach or the FAD-diagram.

The use of these concepts leads to safe predictions of the failure behaviour of wide plates regarding Tgy. The DENT-specimens showed the highest transition temperatures Tgy and the highest constraint in particular for larger 2a/W-ratios whereas the surface notched specimens showed much lower Tgy.

In order to simulate a real structural situation it seems to be justified to test either wide plates with a geometry as similar as possible to the real component to avoid any geometry dependence induced by testing other geometries or to test under severest loading conditions which seemed to be given by DECT-specimens.

Concerning the transition temperature Ti for the onset of stable crack propagation good agreement was found between Ti determined in wide plate tests and Ti determined in fracture mechanics tests. The transfer of Ti from small scale to large scale tests seems to be possible as long as the defect orientation and the plate thickness are equal.

REFERENCES

/1/ Dahl, W. et.al.
ECSC research contract No. 7210-KE/106, Final report, Düsseldorf 1982

/2/ Ehrhardt, H. et.al.
ECSC research contract No. 7210-KE/112, Final report, Düsseldorf 1987

/3/ Miller, A.G.
CEGB-TPRD/B/0093(N82 (Rev 1), London 1984

/4/ Dahl, W. et.al.
Iron and Steel 104 (1984), pp. 909-925

/5/ Rosezin, R.
Dr. Thesis, IEHK, Technical University Aachen 1983

/6/ Ehrhardt, H.
to be published
/7/ Dawes, M.G.
TWI, Report 7803.02/85/461.3, Cambridge 1985
/8/ Dawes, M.G.
Proc. Int. Off. Tech. Conf., Paper No. OTC 5109, pp 267-273
Houston 1986
/9/ BSI, PD 6493, London 1980
/10/ Milne, I. et.al.
CEGB, R/H/R6-Rev. 3, London 1986

C	Si	Mn	P	S	Al	Cu	Cr	Ni
0.20	0.47	1.56	0.021	0.002	0.033	0.070	0.05	0.03

TABLE 1 Chemical composition of the steel

σ_{ys} MPa	σ_{UTS} MPa	A_5 %	Z %	CVN_{max} J	$T_{50\%CVNmax}$ K
401	594	28	75	200	236

TABLE 2 Mechanical properties at room temperature

specimen type	W	2a/W	2c/W	a/t
CNT	300	0.1 0.3 0.5		
CCT	300	0.1		
DENT	300	0.1 0.2 0.3 0.5 0.6 0.8		
	600	0.2 0.8		
SSNT	300		0.2	2/15
			0.37	1/2
			0.5	2/15 1/2 2/3
			1.0	2/15 1/2 2/3

TABLE 3 Geometry of tested wide plates

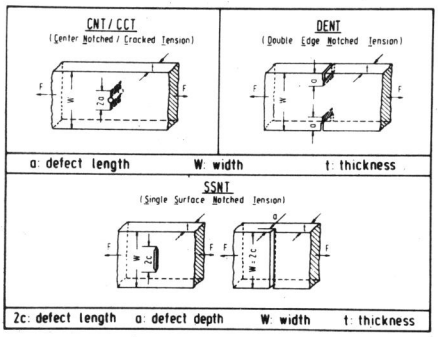

Figure 1 Wide plate design and defect geometry

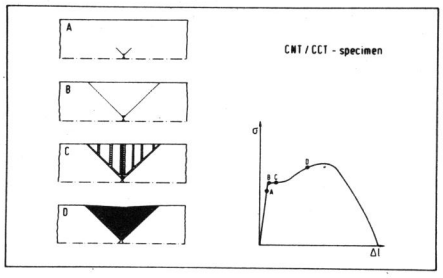

Figure 2 Development of plastic zones in CNT-/CCT-specimens

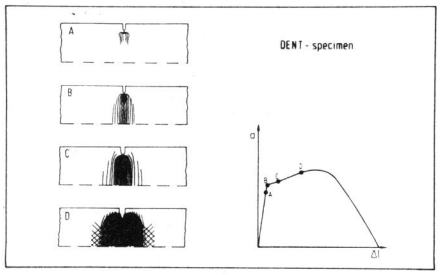

Figure 3 Development of plastic zones in DENT-specimens

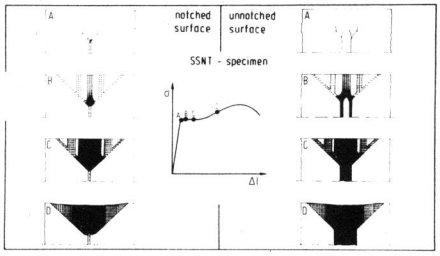

Figure 4 Development of plastic zones in SSNT-specimens

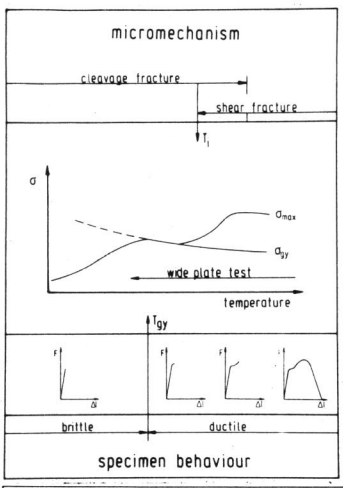

Figure 5 Deformation and fracture behaviour of wide plates as a function of temperature

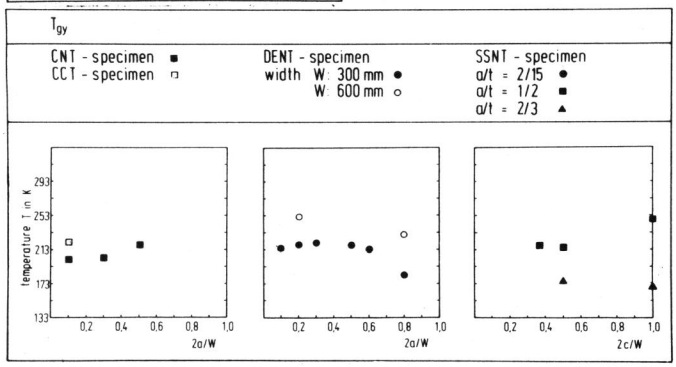

Figure 6 Transition temperature T_{gy} for different specimen types

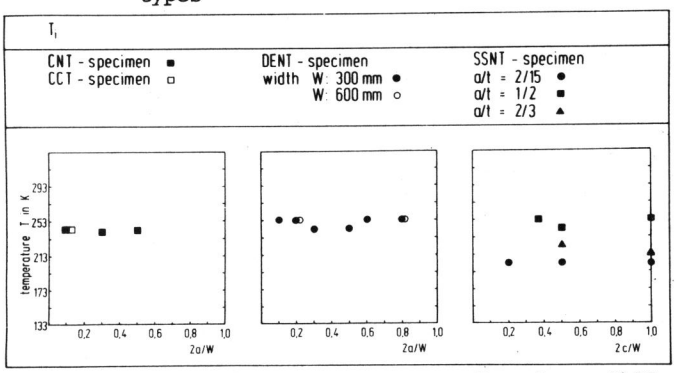

Figure 7 Transition temperature T_i for different specimen types

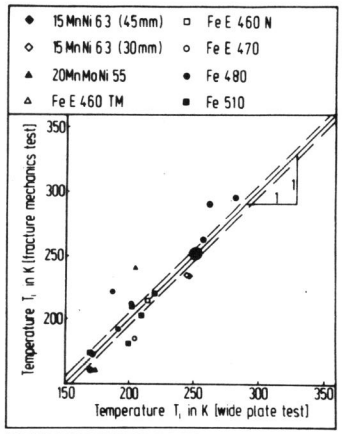

Figure 8

Comparison of transition temperature T_i (fracture mechanics/wide plate)

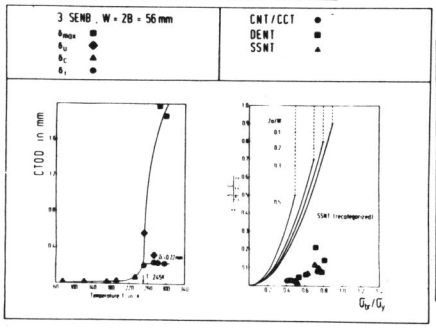

Figure 9 Fracture mechanics properties (CTOD) as a function of temperature (a) and CTOD-Design-Curve-Diagram (b)

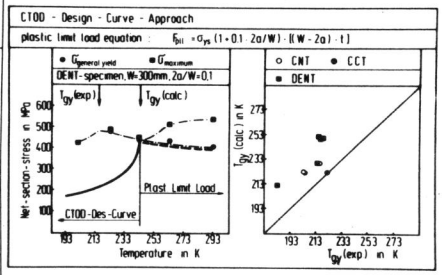

Figure 10 Net-section-stress as a function of temperature (a) and comparison of experimental and calculated T_{gy} (CTOD) (b)

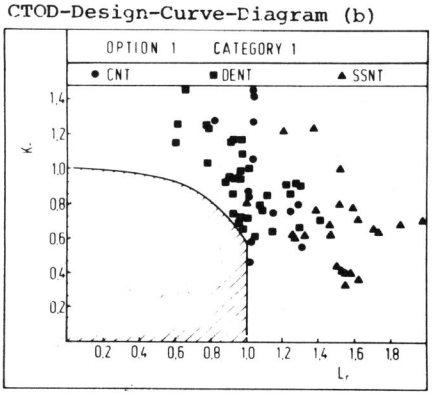

Figure 11 FAD-Diagram (R6-method)

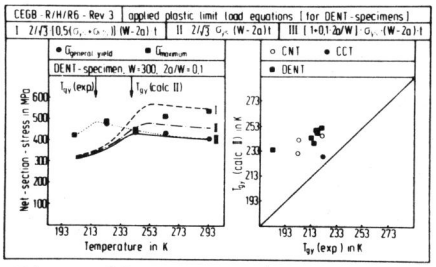

Figure 12 Net-section-stress as a function of temperature (a) and comparison of experimental and calculated T_{gy} (R6-method)